Journal of Affective Disorders 365 (2024) 341–350

Contents lists available at ScienceDirect

Journal of Affective Disorders

journal homepage: www.elsevier.com/locate/jad

Research paper

Unveiling the link between glymphatic function and cortical microstructures in post-traumatic stress disorder

Zhiding Shao [a,1], Xue Gao [a,1], Si Cen [a,1], , for the Department of Defense Alzheimer's Disease Neuroimaging Initiative[2], Xiaolei Tang [b], Juanyu Gong [a,*,1], Wencai Ding [a,*,1]

[a] Department of Neurology, The Second Affiliated Hospital of Wannan Medical College, Wuhu, China
[b] Translational Medicine Center, The Second Affiliated Hospital of Wannan Medical College, Wuhu, China

ARTICLE INFO

Keywords:
Glymphatic system
PTSD
Cortical mean diffusivity
Biomarker

ABSTRACT

Purpose: The discovery of the glymphatic system, crucial for cerebrospinal and interstitial fluid exchange, has enhanced our grasp of brain protein balance and its potential role in neurodegenerative disease prevention and therapy. Detecting early neurodegenerative shifts via noninvasive biomarkers could be key in identifying at-risk individuals for Alzheimer's disease (AD). Our research explores a diffusion tensor imaging (DTI) method that measures cortical mean diffusivity (cMD), potentially a more sensitive indicator of neurodegeneration than traditional macrostructural methods.

Materials and methods: We analyzed 67 post-traumatic stress disorder (PTSD)-diagnosed veterans from the Alzheimer's Disease Neuroimaging Initiative database. Participants underwent structural MRI, DTI, Aβ PET imaging, and cognitive testing. We focused on the DTI-ALPS technique to assess glymphatic function and its relation to cMD, cortical Aβ accumulation, and thickness, accounting for age and APOE ε4 allele variations.

Results: The cohort, all male with an average age of 68.1 (SD 3.4), showed a strong inverse correlation between DTI-ALPS and cMD in AD-affected regions, especially in the entorhinal, parahippocampal, and fusiform areas. Higher DTI-ALPS readings were consistently linked with greater cortical thickness, independent of Aβ deposits and genetic risk factors. Age and cMD emerged as inversely proportional predictors of DTI-ALPS, indicating a complex interaction with age.

Conclusion: The study confirms a meaningful association between glymphatic efficiency and cMD in AD-sensitive zones, accentuating cortical microstructural alterations in PTSD. It positions DTI-ALPS as a viable biomarker for assessing glymphatic function in PTSD, implicating changes in DTI-ALPS as indicative of glymphatic impairment.

1. Introduction

1.1. Glossary

Aβ	amyloid-beta
ADNI	Alzheimer's Disease Neuroimaging Initiative
CDR-SB	Clinical Dementia Rating Scale Sum of Boxes
cMD	cortical mean diffusivity
DTI	diffusion tensor imaging
DTI-ALPS	diffusion tensor image analysis along the perivascular space
FA	fractional anisotropy
MD	mean diffusivity
FSL	FMRIB Software Library 6.0.5
ISF	interstitial fluid
MMSE	Mini-Mental State Examination
PVS	perivascular space
ROI	region of interest
SUVR	standardized uptake value ratio

Post-traumatic stress disorder (PTSD) is a psychiatric disorder that may arise following a traumatic experience, such as military combat

* Correspondence authors.
E-mail addresses: 342531377@qq.com (J. Gong), dingneurology@gmail.com (W. Ding).
[1] These authors contributed equally to this work.
[2] Data used in preparation of this article were obtained from the Alzheimer's Disease Neuroimaging Initiative (ANDI) database (adni.loni.usc.edu). As such, the investigators within the ADNI contributed to the design and implementation of ADNI and/or provided data but did not participate in analysis or writing of this report.

https://doi.org/10.1016/j.jad.2024.08.094
Received 5 December 2023; Received in revised form 16 August 2024; Accepted 17 August 2024
Available online 22 August 2024

(Dohrenwend et al., 2006). Recently, an association was found between PTSD-associated cognitive decline and subsequent Alzheimer's disease (AD) (Song et al., 2020; Roberts et al., 2022). The neuropathology of AD is identified by the accumulation of amyloid-β (Aβ) and tau in the brain (Busche and Hyman, 2020). Therefore, it is crucial that the brain possesses its own mechanism for Aβ and tau clearance. While deposition in peripheral tissues is cleared via the lymphatic veins, the central nervous system (CNS) lacks a traditional lymphatic system (Aukland and Reed, 1993).

Recent studies have demonstrated the existence of a CNS "waste clearance" system, termed as the glymphatic system, which stimulates the recycling of cerebrospinal fluid (CSF) through the brain parenchyma and facilitates the clearance of extracellular solutes including Aβ and tau. (Iliff et al., 2013; Kress et al., 2014; Iliff et al., 2012) In this framework, CSF enters the brain interstitial space from the periarterial space via the astrocytic aquaporin 4-dependent (AQP-4) pathway and subsequently combines with interstitial fluid (ISF) and waste solutes in the brain (Zeppenfeld et al., 2017). The CSF and interstitial fluid subsequently move into the venous perivascular spaces (PVS), causing interstitial fluid flow across the brain parenchyma, thereby removing metabolic waste (Iliff et al., 2012).

Compromised glymphatic and lymphatic drainage systems observed with aging are involved in the accumulation of insoluble tau and Aβ proteins, which contribute to underlying disease processes in neurodegenerative disorders such as AD (Taoka et al., 2017). Recent studies have demonstrated that magnetic resonance imaging (MRI) can be used to measure glymphatic functions, with the majority of these investigations utilizing MRI-tracer-based contrast agents, including gadolinium (Taoka and Naganawa, 2020). However, both intravenous and intrathecal contrast injections are invasive. Despite the growing understanding of glymphatic physiology and pathology, the paucity of non-invasive imaging tools for quantifying glymphatic function hinders the in vivo assessment of glymphatic function (Taoka and Naganawa, 2020).

However, diffusion along the PVS can be assessed using diffusion tensor imaging (DTI) at lower field strengths (Taoka et al., 2017; Taoka et al., 2022; Carotenuto et al., 2022). Diffusion tensor image analysis along the perivascular space (DTI-ALPS) index has been proposed as a less invasive alternative for evaluating glymphatic function (Taoka et al., 2017). In brief, this index is determined from the diffusivity along the deep medullary veins at the level of the lateral ventricles, as an indicator of perivascular clearance activity in brain. Recent research reported a significant correlation between DTI-ALPS and Mini-Mental State Examination (MMSE) scores in AD and mild cognitive impairment (MCI) (Taoka et al., 2017; Kamagata et al., 2022). The DTI-ALPS index has also been observed to decrease with aging in a number of neurodegenerative disorders, such as AD (Kamagata et al., 2022) and Parkinson's disease (McKnight et al., 2021; Ma et al., 2021), compared with healthy participants, ut no study to date has explored this question in adults with PTSD.

Although neurodegeneration is typically indicated in macrostructural alterations, such as cortical thinning as determined by structural MRI, a recent DTI technique, namely cortical mean diffusivity (cMD), has made it possible to evaluate the microstructural features of the gray matter (Montal et al., 2018; Illán-Gala et al., 2019; Rodriguez et al., 2021). The increase in cMD reflects the early disruption of microstructures resulting from damage to cell membranes and dendrites (Weston et al., 2015). Consequently, cMD is a sensitive indicator of cortical microstructural changes that occur before detectable cortical atrophy (Illán-Gala et al., 2019). Recent cross-sectional investigations have found elevated cMD levels in the prodromal and dementia stages of sporadic AD (Montal et al., 2018). Higher cMD has also been shown in AD-signature regions at pathogenic levels of CSF Aβ during the predementia stages of AD (Rodriguez et al., 2021). However, whether DTI-ALPS is associated with cMD and cortical Aβ deposition remains unclear.

Correspondingly, we applied our hypothesis-driven targeted approach to examine the relationships between DTI-ALPS, cMD, and cortical Aβ deposition in a cohort of men with PTSD in relation to neuropsychological tests. We acknowledge the importance of including both Mean MD and FA in DTI analysis. The decision to focus solely on MD was based on the specific characteristics of our study population and recent research. MD provides a more generalized measure of cortical diffusion that is sensitive to microstructural changes in cerebral cortex. Notably, we used surface-based analyses to inspect the main and interactive effects of cMD and cortical Aβ deposition on DTI-ALPS, followed by targeted region of interest (ROI) analyses in AD-vulnerable regions to further confirm their relationships. Additionally, we examined the associations of DTI-ALPS with age, neuropsychological scores, and cortical thickness.

2. Methods

2.1. Study design and participants

The study sample comprised of PTSD veterans from the Brain Aging in Vietnam War Veterans/Department of Defense Alzheimer's Disease Neuroimaging Initiative (DOD-ADNI) database (adni.loni.usc.edu). A longitudinal observational study to characterize the long-term neural and behavioral consequences of post-traumatic stress disorder (PTSD) and/or TBI was carried out. For this study, subjects underwent concurrent T1-weighted MRI, DTI, and [18F]AV45 PET imaging data were selected. All assessments were completed within one year of the T1-weighted MRI scan being taken. Using these inclusion criteria, we obtained a set of participants, all of whom were diagnosed with PTSD using the clinician-administered PTSD scale (CAPS) within DSM-IV (CAPS score > 40). Information on exclusion criteria, and neuropsychological evaluations can be found in the DOD-ADNI database (adni.loni.usc.edu).

2.2. MRI acquisition and processing

All participants underwent a structural three-dimensional T1-weighted spoiled gradient-echo or a magnetization-prepared rapid acquisition with gradient-echo sequence, as well as a DTI sequence on a 3-Tesla scanner using axial spin-echo sequence (detailed acquisition parameters in Supplementary Materials).

In summary, all individuals underwent a T1-weighted scan with a resolution of $1\times 1 \times 1.2$ mm^3 voxels. Scans containing artifacts were eliminated. Images were processed using FreeSurfer (http://surfer.nmr.mgh.harvard.edu, v7.2), normalized to a T1 native surface space, and smoothed with a Gaussian kernel of 15 mm for statistical analysis, as is customary for cortical thickness assessments (Fischl and Dale, 2000).

2.3. Cortical mean diffusivity processing

As previously reported, we estimated cortical mean diffusivity using a surface-based in-house methodology. DTI images were preprocessed using QSIPrep (v0.15.2), which is a containerized pipeline that combines methods from different software and performs important pretreatment steps with the best tools in the field (Cieslak et al., 2021). After N4BiasFieldCorrection, denoising, correction of head motion, eddy currents, and susceptibility distortions, we computed the mean diffusivity metric by fitting a tensor model with the *dtifit* command in the FSL (FMRIB Software Library) (http://fsl.fmrib.ox.ac.uk/fsl/fslwiki, v6.0.5). Subsequently, a $b = 0$ image was registered to a skull-stripped T1-weighted image with a boundary-based algorithm using *a bbregister* (as implemented in FreeSurfer) (Greve and Fischl, 2009). This method accurately registers b0 and T1-weighted images using FreeSurfer's precise segmentation of the white matter and pial surfaces. To create individual cortical mean diffusivity maps, each participant's mean diffusivity volume was sampled at the midpoint of the cortical ribbon and projected it onto each surface that had already been reconstructed

during FreeSurfer processing with the *mri_vol2surf* command. This surface-based method employs recently developed strategies (Coalson et al., 2018; Rodriguez et al., 2021; Montal et al., 2018) to overcome the disadvantages of conventional voxel-based methods. First, it diminishes the influence of white matter and CSF signals on gray matter voxels, which will distort cMD measurements (Jones et al., 2005). Second, a surface vertex-based smoothing approach is utilized, which is less susceptive to the smoothing kernel size than voxel-based analysis (Coalson et al., 2018).

For statistical analyses, all individual cortical mean diffusivity maps were accurately inter-participant matched to a T1 native surface using spherical registration. Across the cortical mantle, we employed a 15-mm two-dimensional full-width half-maximum Gaussian kernel, which is consistent with previous studies on cortical mean diffusivity. The detailed research steps are shown in Fig. 1A.

2.4. DTI analysis along the perivascular space

Individual glymphatic functions were assessed using the DTI-ALPS approach (Taoka et al., 2017). The ALPS technique excels in measuring water diffusivity within perivascular spaces, essential pathways for glymphatic circulation. Unlike conventional DTI metrics that

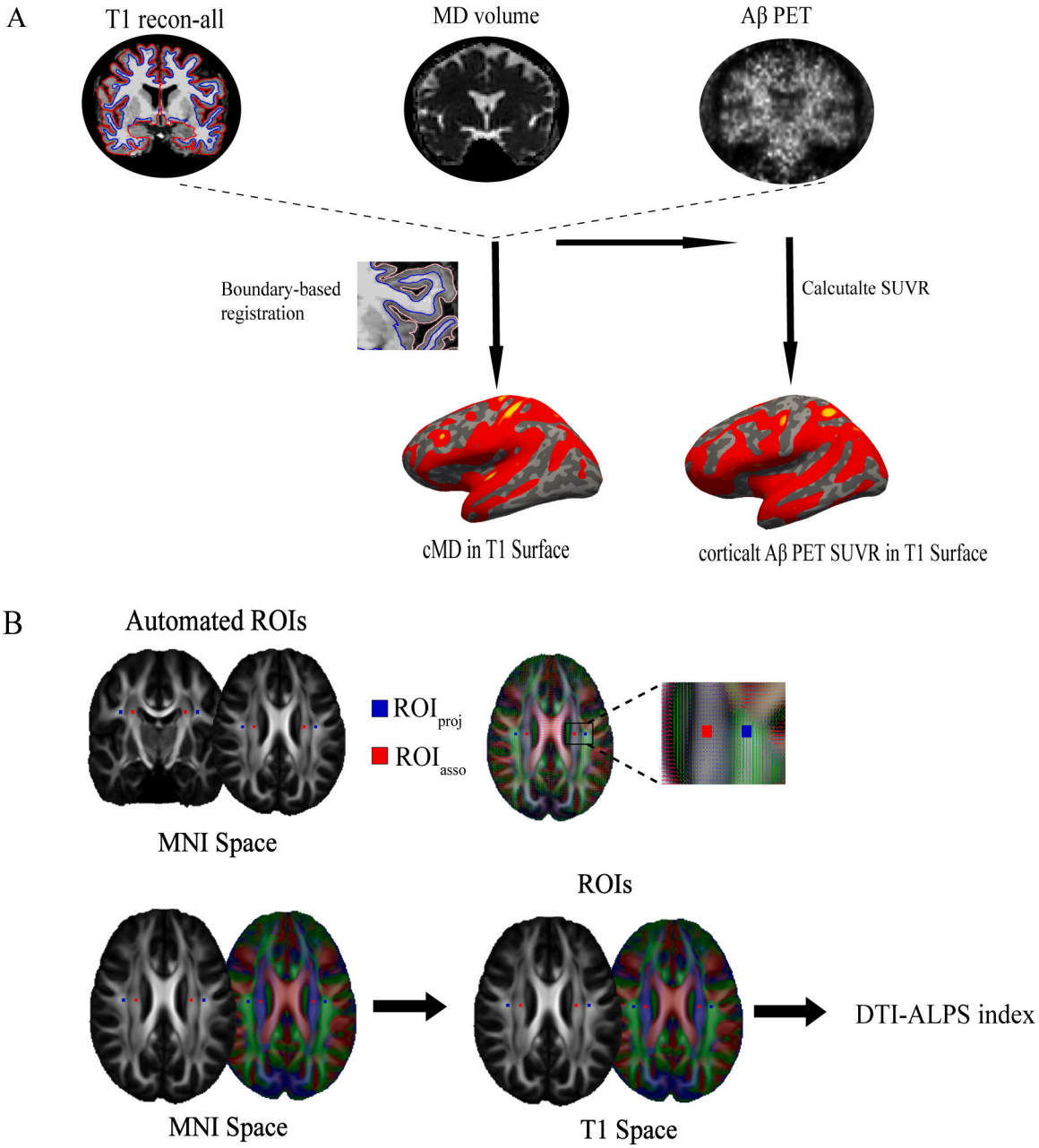

Fig. 1. A. cMD and cortical Aβ PET SUVR pipeline. MD and Aβ PET SUVR volumes were coregistered to the anatomic subject space, projected to the T1 surface. B. MRI processing method for DTI-ALPS calculation. To calculate DTI-ALPS index we first define two ROIs where veins run perpendicular to lateral ventricle using the color-coded FA map in MNI space, two $1 \times 1 \times 1$ mm^3 regions of interest were chosen: one over the area of projection fibers and the other over the area of associative fibers in the bilateral hemispheres. Regions of interest were then registered to the T1 space using the FA map to T1 registration matrix. Then, diffusivities along the x-, y-, and z-axes were extracted for each region of interest. DTI-ALPS was calculated as the ratio of diffusivities perpendicular to fibre bundles and parallel to veins (*Dx proj* and *Dx assoc*) over diffusivities perpendicular to fibre bundles and perpendicular to veins (*Dy proj* and *Dz assoc*). Aβ amyloid-beta, cMD cortical mean diffusivity, DTI-ALPS Diffusion along the perivascular space, FA fractional anisotropy, SUVR standardized uptake value ratio.

may not specifically target these structures, the DTI-ALPS approach provides a precise measure of perivascular space integrity. This precision is crucial given the emerging evidence linking impaired glymphatic function to neurodegenerative conditions. Therefore, DTI-ALPS offers a highly sensitive and focused tool for assessing the functional status of the perivascular spaces, enhancing our understanding of glymphatic system dynamics and its potential disruptions in neurological diseases. This approach analyzes arterial PVS diffusivity on axial slices at the plane of the lateral ventricle bodies. Values are generated using the frame of reference created by diffusion tensor eigenvectors and related eigenvalues. The PVS is nearly perpendicular to both the association and projection fibers. It is represented by the main discrepancies between the x-axis diffusivity in both fibers and the diffusivity perpendicular to both the x-axis and the direction of the fibre tracts. The DTI-ALPS index was determined as the ratio between water diffusivity parallel to vessels (*Dx proj* and *Dx assoc*) and the diffusivities perpendicular to the white matter tracts (*Dy proj* and *Dz assoc*) (Taoka et al., 2017). The following formula was used to calculate the DTI-ALPS index (Taoka et al., 2017):

$$\mathrm{DTI-ALPS} = \frac{\mathrm{mean(Dx\ proj, Dx\ assoc)}}{\mathrm{mean(Dy\ proj, Dz\ assoc)}}$$

Automatic placement of ROIs (T1 space): We calculated the DTI-APLS using two bilateral $1 \times 1 \times 1$ mm^3 ROI placements as recent research has shown this method yields higher reproducibility (Taoka et al., 2022). The two ROIs were automatically placed along the perivascular gap placed on the bilateral association (superior longitudinal fasciculus) and projection (superior and posterior corona radiata) in MNI (Montreal Neurological Institute) standard space. From MNI standard space, all ROIs were subsequently registered in T1 space by exerting the nonlinear Human Connectome Project (HCP) 1065 fractional anisotropy (FA) template to T1 space transformation obtained from the *antsRegistrationSyNQuick.sh* command of the Automatic Normalization Tools (ANTS, http://stnava.github.io/ANTs. v2.2.0). Finally, ROIs were registered to the subject T1 space by using standard FA to the T1 space transformation. To ensure optimal alignment with the perivascular gap, this process involved adjusting the coordinates based on the individual's anatomical variations and confirming the placement through visual inspection by two independent raters to ensure accuracy and consistency. The comprehensive analysis procedure is illustrated in Fig. 1B.

2.5. PET acquisition and processing

Amyloid PET scans were obtained using the radioligand [^{18}F]AV45, which binds to amyloid plaques (acquisition parameters are specified in Supplementary Materials). Primary amyloid PET image analysis was performed in all participants. Motion correction was performed using the *mc-afni2* command in PetSurfer (Greve et al., 2014). The motion-corrected PET volumes were averaged to create a mean PET image file for each participant. Prior to quantification, the mean individual PET volume was co-registered to each individual's native T1 space using *mri_coreg* command in FreeSurfer. Amyloid-PET images were then quantified using cerebellar gray matter as a reference to obtain a partial volume-corrected (PVC) (Greve et al., 2016) standardized uptake value ratio (SUVR), which was projected onto an individual's cortical surface.

2.6. AD signature regions processing

To compare the effects of cMD and cortical Aβ PET SUVR within the same brain regions, six AD-vulnerable ROIs were created using the Desikan atlas (Desikan et al., 2006) in native T1 spaces, which included the bilateral entorhinal, parahippocampal, fusiform, inferior-temporal, middle-temporal, and orbito-frontal gyri. Using data-driven, postmortem (Braak and Braak, 1991), and in vivo staging techniques, these regions of interest (ROI) are typically characterized as sensitive to cortical thinning (Schwarz et al., 2016), cMD alternation (Montal et al., 2018), and Aβ aggregation (Sepulcre et al., 2017; Tosun et al., 2017). Then, cMD diffusivity and cortical Aβ were extracted from these AD signature ROIs.

2.7. Statistical analysis

Surface vertex-based analyses: To determine the associations of Aβ PET SUVR, cortical microstructure and cortical thickness with DTI-ALPS, we performed a vertex-wise partial correlation analysis between cMD, cortical Aβ, and DTI-APLS. Age and APOE ε4 status were covariates. To avoid false positives, a Monte Carlo simulation with 10,000 repetitions (family wise error [FWE], $P < 0.05$) was used. The Supplementary data contains further information.

The ability of localized cMD and cortical Aβ burden to predict DTI-APLS was independently evaluated using regional multivariable regression. We used univariate linear regression to model the associations between DTI-ALPS and participant characteristics as well as the time of day when MRI scans, cMD, and Aβ PET were performed. The main effects linear regression model included DTI-ALPS as an independent variable according to the following formula:

$$\mathrm{DTI-ALPS} = \beta_0 + \beta_1{*}\mathrm{Age} + \beta_2{*}\mathrm{APOE}\ \varepsilon4 + \beta_3{*}\mathrm{cMD} + \beta_4{*}\mathrm{cortical}\ A\beta\ PET\ SUVR + \varepsilon.$$

In addition, models were generated to detect the interaction between regional cMD and cortical Aβ burden in predicting DTI-ALPS and their respective independent contributions.

When comparing the statistical fit of several models using the Akaike information criterion (AIC) and *R* (Song et al., *2020*), the lowest AIC value implies a better fit. All models included APOE ε4 status and age as covariates.

3. Results

3.1. Participant characteristics

We included 86 patients with PTSD. Six participants were excluded from the study due to having an unknown APOE ε4 status. Of the 80 participants, 74 (92.5 %) completed MRI and [^{18}F]AV45 PET imaging. A total of 5 participants (93.2 %) did not undergo comprehensive neuropsychological testing and were excluded from the study. Two participants had registration failures found during pre-processing of MRI and were also excluded. Following imaging processing and quality control, data from 67 male participants (mean age of 68.1 ± 3.4 years [years ± SD]) were available for DTI-ALPS analysis (flowchart in Fig. 2). The demographic, clinical, and neuropsychological characteristics of the participants are summarized in Table 1.

3.2. Partial correlation analyses between DTI-ALPS, cMD, and cortical Aβ PET SUVR

3.2.1. Whole-brain vertex-wise analyses

The associations of DTI-ALPS with vertex-wise cMD were localized in the parahippocampal, fusiform, and lingual gyri in the bilateral hemisphere and in the entorhinal cortex in the right hemisphere (Fig. 3A). These relationships were verifid when ROI-based analyses were performed on bilateral cMD ROIs (Table S1). Entorhinal cMD had the strongest negative association with DTI-ALPS, with the regression models accounting for approximately 31 % of the total variance in DTI-ALPS (Std. $\beta = -9.83$, 95 % CI -10.73 to −8.94, $P = 0.00023$; Table S1). No significant partial correlation was found between DTI-ALPS and vertex-wise cortical Aβ PET SUVR (Fig. 3B). When ROI-based analyses were applied to bilateral cortical Aβ PET SUVR, no correlations were shown with DTI-ALPS (not shown). APOE ε4 status and age were taken into account in partial correlation analyses. All the analyses are adjusted by age and APOE ε4 status.

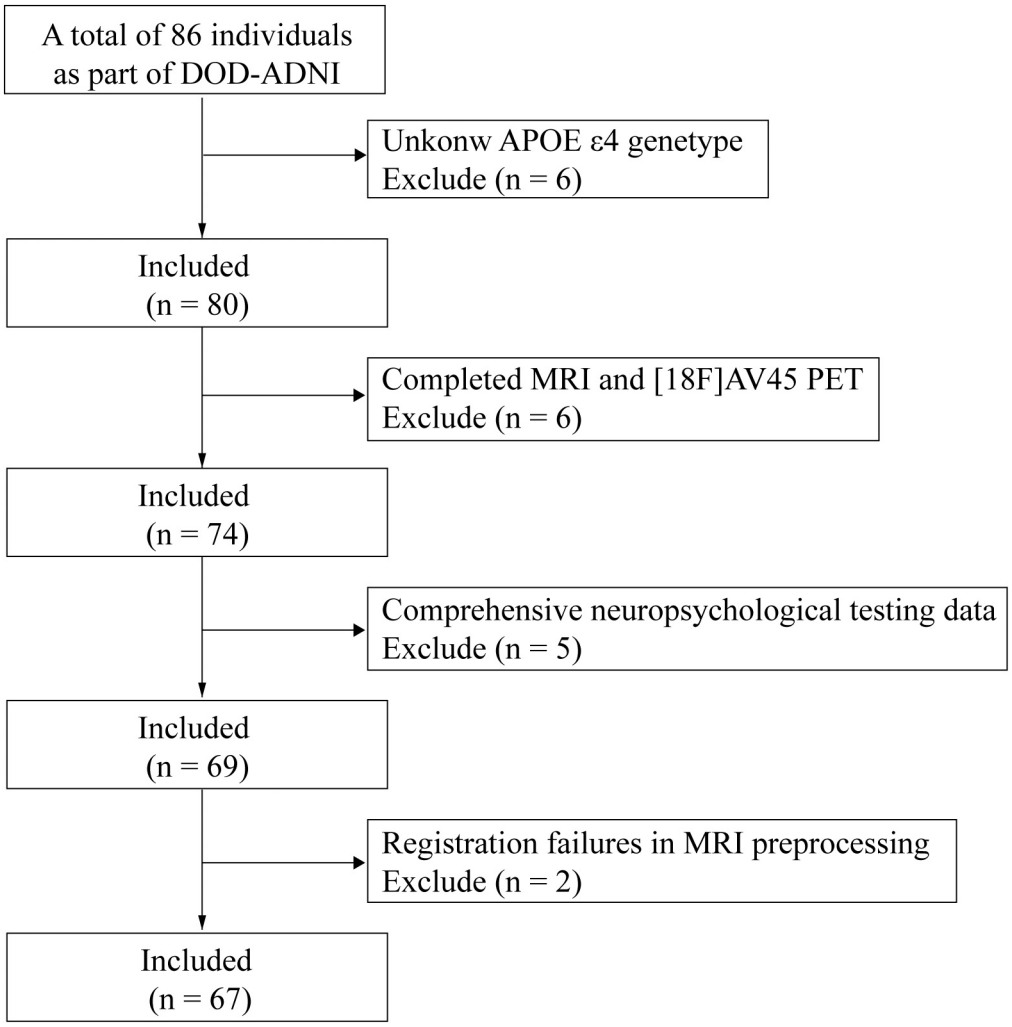

Fig. 2. Flow Chart of the Inclusion Process. *n*, number of patients.

3.2.2. AD signature regions analyses

DTI-ALPS was significantly negatively correlated with cMD in all participants in the AD signature regions, especially in the entorhinal, parahippocampal, and fusiform gyri (Fig. 4). Here are ROI-based scatterplots for the entorhinal, parahippocampal, and fusiform regions. (Fig. 4). Age was also found to have a substantial negative connection with DTI-ALPS in the entorhinal and parahippocampal gyri (Fig. 4A and B). There was an observational significant interaction between age and regional cMD in predicting DTI-ALPS, as shown in Fig. 4A and Fig. 4B, for cMD in the entorhinal and parahippocampal regions, respectively. The individual terms for regional cMD (entorhinal and parahippocampal) remained significant independent predictors of DTI-ALPS in these interaction models. (Table 2). These findings were confirmed in the subsequent ROI analysis (Table 2). Entorhinal cMD had the strongest negative relationship with DTI-ALPS, contributing to approximately 30 % of the overall variance in DTI-ALPS (Std. $\beta = -10.02$, 95 % CI -10.93 to −9.11, $P = 0.00021$; Table 2). Parahippocampal cMD showed the strongest negative relationship with DTI-ALPS, accounting for approximately 26 % of the total variance in DTI-ALPS (Std. $\beta = -6.87$, 95 % CI -7.83 to −5.91, $P = 0.00064$; Table 2). We noticed an obvious interaction between cMD and age for predicting DTI-ALPS, which was significant in the entorhinal (Std. $\beta = 11.91$, 95 % CI 11.89 to 11.92, $P = 0.00038$; Table 2) and parahippocampal regions (Std. $\beta = 8.52$, 95 % CI 8.43 to 11.24, $P = 0.01$; Table 2). Cortical PET SUVR and cMD did not interact significantly in predicting DTI-ALPS (data not shown). There was no predictive value for DTI-ALPS in the inferior-temporal, middle-temporal, or orbitofrontal gyri for any of these regional cMD values.

3.3. Associations between DTI-ALPS and cortical thickness

After removing the effects APOE ε4 status and age, we found that higher a DTI-ALPS was associated with a higher cortical thickness, mainly in the left entorhinal gyrus, parahippocampal gyrus, and fusiform gyrus (Fig. S1).

4. Discussion

In this study, we used a non-invasive diffusion-derived MRI index of diffusivity along the PVS, called the DTI-ALPS, to investigate in vivo glymphatic system function in a cohort of PTSD veterans. First, we showed that advancing age and higher regional cMD, but not regional Aβ PET SUVR, were independent factors associated with lower glymphatic dysfunction as reflected by the DTI-ALPS index. Second, we noticed a evident interaction between cMD and age in predicting the DTI-ALPS. Third, we found that a lower DTI-ALPS index was closely related to lower cortical thickness and impaired neuropsychological test performance, even when age and APOE ε4 status were considered, possibly due to impaired glymphatic system functioning.

Using a surface-based approach we identified, for the first time, a significant negative correlation between DTI-ALPS and cMD in PTSD veterans. Previous studies have proposed that the glymphatic system may provide a clearance mechanism for protein species, such as Aβ and

Table 1
Demographic and laboratory characteristics of 67 participants.

Characteristics	Values
Demographic	
Age (years)	68.1 (3.4)
Education (years)	14.4 (2.4)
Sex (male)	67 (100 %)
Clinical	
APOE ε4 status	
Negative	53 (79.1 %)
Positive	14 (20.9 %)
Clinician-administered PTSD scale scores	
Current	57.3 (13.1)
Life	74.0 (18.5)
Neuropsychological Performance	
ADAS-Cog	12.9 (4.0)
CDR-SB	0.2 (0.3)
CES	24.2 (10.1)
MoCA	25.2 (2.3)
MMSE	28.0 (1.6)
GDS	4.3 (3.2)
ECog Memory	2.3 (0.7)
ECog Language	2.1 (0.8)
ECog Spatial Visual	1.5 (0.6)
ECog Plan	1.7 (0.9)
ECog Organize	2.0 (1.0)
ECog Divide Attention	2.1 (0.9)
ECog total	2.0 (0.7)
Glymphatic Function	
DTI-ALPS	1.3 (0.2)

ADAS-Cog = cognitive subscale of the Alzheimer's Disease Assessment Scale; APOE = apolipoprotein; CDR-SB = Clinical Dementia Rating Scale Sum of Boxes; CES = Combat Exposure Score; DTI-ALPS = diffusion tensor image analysis along the perivascular space; ECog = Everyday Cognition; GDS = Geriatric Depression Scale; MoCA = Montreal Cognitive Assessment; MMSE = Mini Mental State Exam.

tau, which accumulate in the brain in AD (Zeppenfeld et al., 2017; Harrison et al., 2020). The poor performance of this system raises the possibility that decreased glycolytic clearance contributes to the susceptibility of the aging brain to aberrant protein accumulation (Kress et al., 2014). Meanwhile, cMD is a more sensitive novel biomarker than cortical thickness for the early detection of neurodegeneration-related microstructural changes in diseases such as AD and frontotemporal dementia (Montal et al., 2018; Illán-Gala et al., 2019). It can also be a standalone predictor of cognitive impairment, neurodegeneration, and clinical aggravation in older adults (Rodriguez et al., 2021). The AD regional signature cMD was able to predict DTI-ALPS significantly after adjusting for regional Aβ burden, age, and APOE ε4 status. Considering its correlation with cortical thickness, it indicates a close correlation between DTI-ALPS and cMD. Moreover, cMD can independently explain the variance in DTI-ALPS beyond traditional imaging biomarkers. Importantly, the regions where higher cMD was predictive of decreased DTI-ALPS, independent of Aβ PET SUVR, were consistent with regions experiencing early tau aggregation and deposition (transentorhinal and limbic regions), which was in line with Braak and Braak (Braak and Braak, 1997) stages I–II or Delacourte (Delacourte et al., 1999) stages 1–3. Taking into account previous studies, our research confirms the hypothesis that cMD is an early biomarker of DTI-ALPS and that tau driven synaptic disfunction precedes apparent neuronal damage and cortical thinning. Higher cMD without cortical thinning may indicate slightly earlier DTI-ALPS and microstructural impairment in response to tau (Villemagne et al., 2015). This results in synaptic dysfunction and toxicity that occurs prior to neuronal necrosis, as proved by preclinical research as well as deposition of other protein oligomers (Busche and Hyman, 2020). Our observations showed no correlation between DTI-ALPS scores and the severity of cortical Aβ deposition. Multiple findings have demonstrated Aβ aggregation alone is clearly insufficient to cause symptoms of AD (Chételat et al., 2013; Sperling et al., 2011), and current research has confirmed that both Aβ and tau are essential for cognitive impairment in healthy participants (Betthauser et al., 2020; Jack et al., 2019). The lack of a significant correlation between DTI-ALPS and cortical Aβ deposition in our study aligns with the understanding that Aβ alone may not be sufficient to drive cerebral impairment. Instead, our findings suggest that cMD, as an early marker of microstructural changes, is more closely related to tau pathology, which precedes observable neuronal damage and cortical thinning. Regions with higher cMD, independent of Aβ burden, correspond to areas of early tau aggregation, indicating that cMD might be an early indicator of tau-related dysfunction. This supports the view that tau-driven synaptic dysfunction, rather than Aβ deposition, plays a more critical role in the progression of neurodegeneration observed in PTSD and other neurodegenerative conditions. However, no studies have examined the risk of cortical amyloid-β deposition in DTI-ALPS. Future longitudinal studies are needed to clarify this potential association.

Our results confirm a significant correlation between DTI-ALPS and age, as revealed through the independent cohorts. The relationship between advancing age and DTI-ALPS has already been demonstrated in several cohorts of community-dwelling older adults (Siow et al., 2022), in different stages of Parkinson's disease (McKnight et al., 2021; Ma

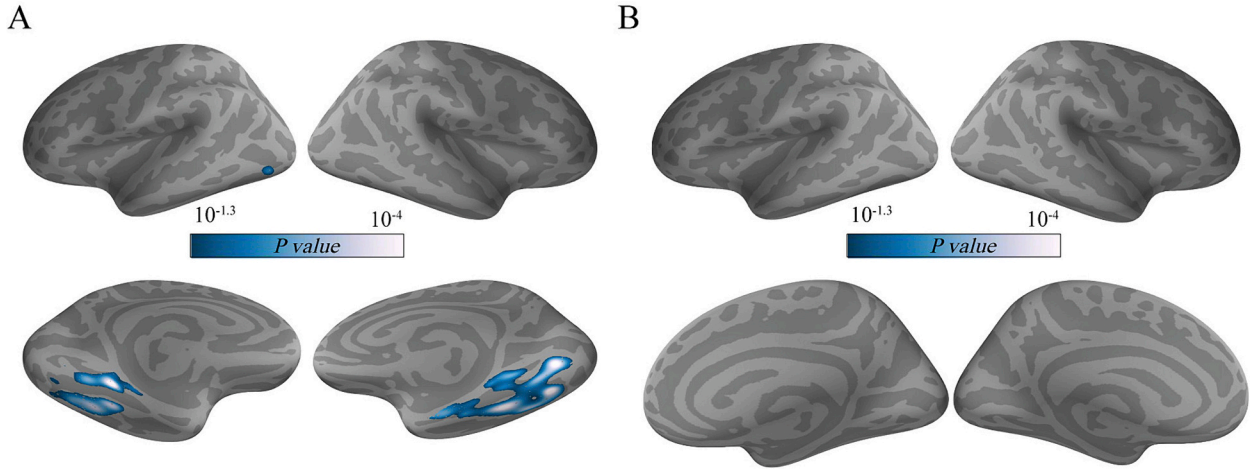

Fig. 3. Associations of DTI-ALPS with whole brain vertex-wise cMD. A Surface-based statistical map of clusters with significant association between DTI-ALPS and vertex-wise cMD. Clusters survived multiple comparison correction by employing a cluster extension requirement in a Monte Carlo simulation with 10,000 iterations. B No significant partial correlation was noted between DTI-ALPS and vertex-wise cortical Aβ PET SUVR. All the analyses are adjusted by age and APOE ε4 status. Aβ amyloid-beta, cMD cortical mean diffusivity, DTI-ALPS diffusion tensor imaging-analysis along the perivascular space, SUVR standardized uptake value ratio.

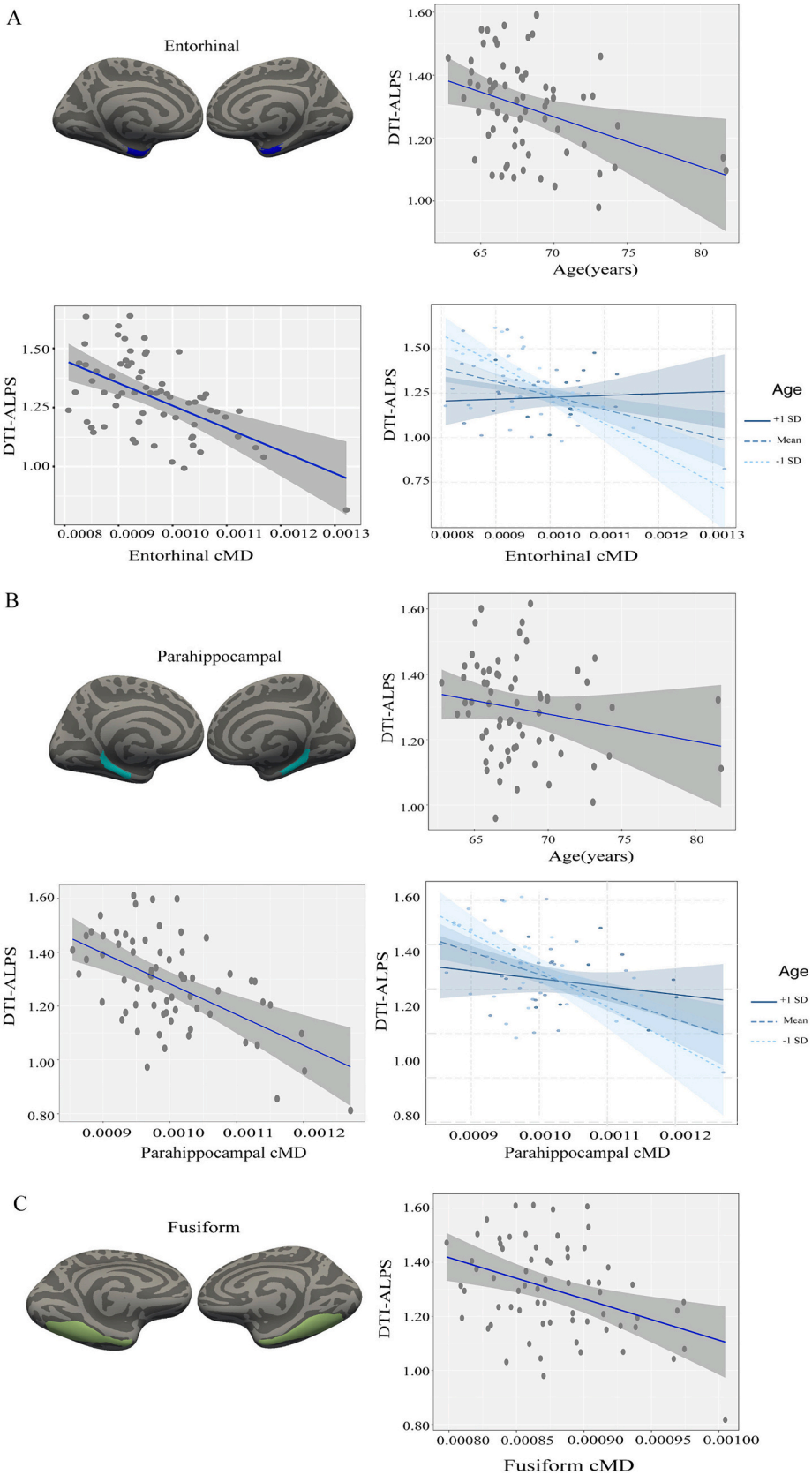

Fig. 4. Associations of DTI-ALPS with cMD and age. A. Association of DTI-ALPS with cMD and age and the significant interaction between entorhinal cMD and age. B. The relationship between DTI-ALPS and parahippocampal cMD and the significant interaction between parahippocampal cMD and age. C. The correlation between DTI-ALPS and fusiform cMD. All the correlation analyses were adjusted for APOE ε4 status. cMD cortical mean diffusivity, DTI-ALPS diffusion tensor imaging-analysis along the perivascular space.

Table 2
Multivariable regression models predicting the DTI-ALPS.

Indep. pred.	Std. β (95 % CI)	*P* value	R^2(AIC)
DTI-ALPS ~ Age + ApoE4 + Entorhinal cMD + Entorhinal Aβ-PET SUVR + Age*Entorhinal cMD			
Age	−5.20 (−5.34 to −5.07)	3.34×10^{-4}	0.30 (−62.21)
APOE ε4 (+)	−0.20 (−0.29 to −0.11)	6.88×10^{-2}	
Entorhinal cMD	−10.02 (−10.93 to −9.11)	2.14×10^{-4}	
Entorhinal Aβ-PET SUVR	−0.08 (−0.26 to 0.10)	0.48	
Age*Entorhinal cMD	11.91 (11.89 to 11.92)	3.80×10^{-4}	
DTI-ALPS ~ Age + ApoE4 + Entorhinal cMD + Entorhinal Aβ-PET SUVR			
Age	−0.07 (−0.08 to −0.06)	0.56	0.16 (−50.22)
APOE ε4 (+)	−0.20 (−0.31 to −0.11)	8.88×10^{-2}	
Entorhinal cMD	−0.45 (−5.02 to 4.11)	7.61×10^{-4}	
Entorhinal Aβ-PET SUVR	−0.04 (−0.24 to 0.15)	0.73	
DTI-ALPS ~ Age + ApoE4 + Parahippocampal cMD + Parahippocampal Aβ-PET SUVR + Age*Parahippocampal cMD			
Age	−3.93 (−4.08 to −3.79)	0.01	0.26 (−57.85)
APOE ε4 (+)	−0.12 (−0.22 to −0.02)	0.29	
Parahippocampal cMD	−6.87 (−7.83 to −5.91)	6.04×10^{-3}	
Parahippocampal Aβ-PET SUVR	−0.11 (−0.27 to 0.05)	0.36	
Age* Parahippocampal cMD	8.52 (8.43 to 11.24)	0.01	
DTI-ALPS ~ Age + ApoE4 + Parahippocampal cMD + Parahippocampal Aβ-PET SUVR			
Age	-9.87×10^{-4} (−0.01 to 0.01)	0.99	0.18 (−52.59)
APOE ε4 (+)	−0.13(−0.23 to −0.03)	0.26	
Parahippocampal cMD	−0.5 (−5.54 to 4.55)	2.1×10^{-4}	
Parahippocampal Aβ-PET SUVR	−0.08 (−0.25 to 0.09)	0.51	
DTI-ALPS ~ Age + ApoE4 + Fusiform cMD + Fusiform Aβ-PET SUVR			
Age	−0.08 (−0.09 to −0.07)	0.50	0.12 (−47.53)
APOE ε4 (+)	−0.09 (−0.20 to 0.01)	0.46	
Fusiform cMD	−0.39 (−10.05 to 9.26)	2.43×10^{-3}	
Fusiform Aβ-PET SUVR	−0.06 (−0.24 to 0.12)	0.64	

et al., 2021), and in newly diagnosed focal epilepsy (Lee et al., 2022). These results are consistent with our study showing that advancing age correlates with the deterioration of glymphatic function, suggesting that other age-related alterations may be involved. Studies investigating the glymphatic system in aged mice revealed that loss of perivascular AQP4 polarization and decreased vascular wall pulsatility may lead to impaired Aβ clearance and inefficient exchange between the subarachnoid CSF and brain parenchyma (Kress et al., 2014). This could explain the independent relationship between age and decreased DTI-ALPS scores reported in our study.

The current study suggests that the interaction between cMD and age may play a role in DTI-ALPS degradation. Specifically, we observed that greater cMD was associated with lower DTI-ALPS but only with age. One possible explanation is that this cohort comprised individuals within a narrow age range and lacked a group comprising younger individuals. This suggests that for older individuals with PTSD, cMD may serve as a potential marker for identifying participants at an increased risk of DTI-ALPS deterioration and progression of clinical symptoms, which may be useful for preventative trials.

Our findings from the gray matter cortical thickness analyses were consistent with the relationships between DTI-ALPS and neuropsychological test scores. Significant correlations between lower DTI-ALPS and greater gray matter cortical thickness were observed in several brain regions known to be involved in cognitive processing (e.g., the entorhinal, parahippocampal, fusiform, and inferior temporal gyri). A recent study involving Aβ and tau-specific PET tracers found that in in vivo entorhinal and parahippocampal gyri, tau deposition is related with the performance of episodic memory and medial temporal lobe atrophy in cognitively healthy individuals independent of Aβ (Maass et al., 2018). Moreover, the DTI-ALPS index is a valuable biomarker for assessing tau deposition (Ota et al., 2022). Consistent with this insight, our findings indicate that the entorhinal and parahippocampal gyri are vulnerable to glymphatic dysfunction.

Our analysis revealed that cMD exhibited a broader range and more significant changes compared to cortical thickness. Specifically, higher cMD values, as measured by DTI-ALPS, were more consistently and significantly associated with areas of the brain exhibiting neurodegenerative changes. In contrast, the changes in cortical thickness were less pronounced and showed a narrower range of statistical significance. Importantly, we found that changes in cMD identified by DTI-ALPS not only corresponded with regions showing altered cortical thickness but also extended to more extensive bilateral symmetrical areas. This indicates that cMD changes reflect a more comprehensive pattern of microstructural alterations compared to cortical thickness alone.

This study has several limitations. First, it is challenging to determine the timing of the structural changes in the brain that accompany PTSD because of the intensity of the initial trauma and the age at which the symptoms first appear. Second, our research is cross-sectional; hence, it lacks longitudinal data on DTI-ALPS temporal changes, cMD alternations, rate of Aβ deposition, and changes in cognitive performance over time. Third, DTI-ALPS cannot assess whole-brain glymphatic performance; it relies on the projection of the lateral ventricular body and orthogonal geometric correlation between the connecting fibers, medullary arteries, and veins. Finally, its cross-sectional design prevented us from drawing any conclusions on the dynamics of glymphatic impairment in PTSD and the temporal definition of the interaction among glymphatic system impairment, cortical microstructural abnormalities, and cortical Aβ deposition. Longitudinal investigative studies should strongly be advocated to explore the potential usefulness of glymphatic function evaluation as a biomarker of illness development in progressive disease stages.

Our analyses implicate aging and cMD in PTSD glymphatic function by revealing that advancing age and higher cMD are independent variables that correspond to a lower DTI-ALPS index. However, additional studies are required to validate this DTI-ALPS approach. Our research also found relationships between impaired DTI-ALPS and reduced gray matter cortical thickness, suggesting that DTI-ALPS may serve as a biomarker for detecting and monitoring cognitive impairment in PTSD. Our results suggest a strong relationship between glymphatic function, aging, cMD, and cognition. Further research is required to clarify the pathophysiological correlates and clinical significance of this finding.

Author contributions

WCD and ZDS contributed to the conception and design of the study; WCD, ZDS, XG, and SC contributed to the acquisition and analysis of data; WCD, ZDS, XLT and JYG contributed to drafting the text or preparing the figures.

Funding

No funding was received.

Availability of data and materials

Data used in preparation of this article were obtained from the Alzheimer's Disease Neuroimaging Initiative (ADNI) database (adni.loni.usc.edu).

Ethics approval and consent to participants

The protocol, patient information, consent form, and other relevant study documentation were approved by the institutional review boards of all participants sites within ADNI and written informed consent was obtained for all study. The studies were performed in accordance with the Declaration of Helsinki.

Consent for publication

All participants in this study have provided consent for their de-identifed data to contribute to publication of the research findings.

CRediT authorship contribution statement

Zhiding Shao: Writing – review & editing, Methodology, Investigation, Formal analysis. **Xue Gao:** Funding acquisition, Formal analysis. **Si Cen:** Investigation. **Xiaolei Tang:** Software. **Juanyu Gong:** Supervision. **Wencai Ding:** Writing – review & editing, Visualization, Supervision, Software, Resources, Formal analysis, Conceptualization.

Declaration of competing interest

The authors declare that they have no competing interests.

Acknowledgements

The authors acknowledge DOD-ADNI contributors listed at http://adni.loni.usc.edu/data-samples/access-data/groups-acknowledgements-journal-format/. Data used in preparation of this article were obtained from the ADNI database (http://adni.loni.usc.edu). The ADNI investigators provided data and/or were involved in the design and implementation of the ADNI, but they did not take part in the analysis or writing of this report. A complete listing of ADNI investigators can be found at: http://adni.loni.usc.edu/wp-content/uploads/how_to_apply/ADNI_Acknowledgement_List.pdf

Appendix A. Supplementary data

Supplementary data to this article can be found online at https://doi.org/10.1016/j.jad.2024.08.094.

References

Aukland, K., Reed, R.K., 1993. Interstitial-lymphatic mechanisms in the control of extracellular fluid volume. Physiol. Rev. 73, 1–78.
Betthauser, T.J., Koscik, R.L., Jonaitis, E.M., et al., 2020. Amyloid and tau imaging biomarkers explain cognitive decline from late middle-age. Brain 143, 320–335.
Braak, H., Braak, E., 1991. Neuropathological stageing of Alzheimer-related changes. Acta Neuropathol. 82, 239–259.
Braak, H., Braak, E., 1997. Frequency of stages of Alzheimer-related lesions in different age categories. Neurobiol. Aging 18, 351–357.
Busche, M.A., Hyman, B.T., 2020. Synergy between amyloid-β and tau in Alzheimer's disease. Nat. Neurosci. 23, 1183–1193.
Carotenuto, A., Cacciaguerra, L., Pagani, E., Preziosa, P., Filippi, M., Rocca, M.A., 2022. Glymphatic system impairment in multiple sclerosis: relation with brain damage and disability. Brain 145, 2785–2795.
Chételat, G., la Joie, R., Villain, N., et al., 2013. Amyloid imaging in cognitively normal individuals, at-risk populations and preclinical Alzheimer's disease. Neuroimage Clin. 2, 356–365.
Cieslak, M., Cook, P.A., He, X., et al., 2021. QSIPrep: an integrative platform for preprocessing and reconstructing diffusion MRI data. Nat. Methods 18, 775–778.
Coalson, T.S., van Essen, D.C., Glasser, M.F., 2018. The impact of traditional neuroimaging methods on the spatial localization of cortical areas. Proc. Natl. Acad. Sci. USA 115, E6356–E6365.
Delacourte, A., David, J.P., Sergeant, N., et al., 1999. The biochemical pathway of neurofibrillary degeneration in aging and Alzheimer's disease. Neurology 52, 1158–1165.
Desikan, R.S., Ségonne, F., Fischl, B., et al., 2006. An automated labeling system for subdividing the human cerebral cortex on MRI scans into gyral based regions of interest. Neuroimage 31, 968–980.
Dohrenwend, B.P., Turner, J.B., Turse, N.A., Adams, B.G., Koenen, K.C., Marshall, R., 2006. The psychological risks of Vietnam for U.S. veterans: a revisit with new data and methods. Science 313, 979–982.
Fischl, B., Dale, A.M., 2000. Measuring the thickness of the human cerebral cortex from magnetic resonance images. Proc. Natl. Acad. Sci. USA 97, 11050–11055.
Greve, D.N., Fischl, B., 2009. Accurate and robust brain image alignment using boundary-based registration. Neuroimage 48, 63–72.
Greve, D.N., Svarer, C., Fisher, P.M., et al., 2014. Cortical surface-based analysis reduces bias and variance in kinetic modeling of brain PET data. Neuroimage 92, 225–236.
Greve, D.N., Salat, D.H., Bowen, S.L., et al., 2016. Different partial volume correction methods lead to different conclusions: an (18)F-FDG-PET study of aging. Neuroimage 132, 334–343.
Harrison, I.F., Ismail, O., Machhada, A., et al., 2020. Impaired glymphatic function and clearance of tau in an Alzheimer's disease model. Brain 143, 2576–2593.
Iliff, J.J., Wang, M., Liao, Y., et al., 2012. A paravascular pathway facilitates CSF flow through the brain parenchyma and the clearance of interstitial solutes, including amyloid β. Sci. Transl. Med. 4, 147ra111.
Iliff, J.J., Lee, H., Yu, M., et al., 2013. Brain-wide pathway for waste clearance captured by contrast-enhanced MRI. J. Clin. Invest. 123, 1299–1309.
Illán-Gala, I., Montal, V., Borrego-Écija, S., et al., 2019. Cortical microstructure in the behavioural variant of frontotemporal dementia: looking beyond atrophy. Brain 142, 1121–1133.
Jack, C.R., Wiste, H.J., Therneau, T.M., et al., 2019. Associations of amyloid, tau, and neurodegeneration biomarker profiles with rates of memory decline among individuals without dementia. JAMA 321, 2316–2325.
Jones, D.K., Symms, M.R., Cercignani, M., Howard, R.J., 2005. The effect of filter size on VBM analyses of DT-MRI data. Neuroimage 26, 546–554.
Kamagata, K., Andica, C., Takabayashi, K., et al., 2022 Sep 19. Association of MRI indices of glymphatic system with amyloid deposition and cognition in mild cognitive impairment and Alzheimer disease. Neurology, Epub.
Kress, B.T., Iliff, J.J., Xia, M., et al., 2014. Impairment of paravascular clearance pathways in the aging brain. Ann. Neurol. 76, 845–861.
Lee, D.A., Park, B.S., Ko, J., et al., 2022. Glymphatic system function in patients with newly diagnosed focal epilepsy. Brain Behav. 12, e2504.
Ma, X., Li, S., Li, C., et al., 2021. Diffusion tensor imaging along the perivascular space index in different stages of Parkinson's disease. Front. Aging Neurosci. 13, 773951.
Maass, A., Lockhart, S.N., Harrison, T.M., et al., 2018. Entorhinal tau pathology, episodic memory decline, and neurodegeneration in aging. J. Neurosci. 38, 530–543.
McKnight, C.D., Trujillo, P., Lopez, A.M., et al., 2021. Diffusion along perivascular spaces reveals evidence supportive of glymphatic function impairment in Parkinson disease. Parkinsonism Relat. Disord. 89, 98–104.
Montal, V., Vilaplana, E., Alcolea, D., et al., 2018. Cortical microstructural changes along the Alzheimer's disease continuum. Alzheimers Dement. 14, 340–351.
Ota, M., Sato, N., Nakaya, M., et al., 2022 Sep 15. Relationships between the deposition of amyloid-β and tau protein and glymphatic system activity in Alzheimer's disease: diffusion tensor image study. J Alzheimers Dis, Epub.
Roberts, A.L., Liu, J., Lawn, R.B., et al., 2022. Association of Posttraumatic Stress Disorder with Accelerated Cognitive Decline in middle-aged women. JAMA Netw. Open 5, e2217698.
Rodriguez-Vieitez, E., Montal, V., Sepulcre, J., et al., 2021. Association of cortical microstructure with amyloid-β and tau: impact on cognitive decline, neurodegeneration, and clinical progression in older adults. Mol. Psychiatry 26, 7813–7822.
Schwarz, C.G., Gunter, J.L., Wiste, H.J., et al., 2016. A large-scale comparison of cortical thickness and volume methods for measuring Alzheimer's disease severity. Neuroimage Clin. 11, 802–812.
Sepulcre, J., Grothe, M.J., Sabuncu, M., et al., 2017. Hierarchical Organization of tau and Amyloid Deposits in the cerebral cortex. JAMA Neurol. 74, 813–820.
Siow, T.Y., Toh, C.H., Hsu, J.-L., et al., 2022. Association of Sleep, neuropsychological performance, and gray matter volume with Glymphatic function in community-dwelling older adults. Neurology 98, e829–e838.
Song, H., Sieurin, J., Wirdefeldt, K., et al., 2020. Association of Stress-Related Disorders with Subsequent Neurodegenerative Diseases. JAMA Neurol. 77, 700–709.
Sperling, R.A., Aisen, P.S., Beckett, L.A., et al., 2011. Toward defining the preclinical stages of Alzheimer's disease: recommendations from the National Institute on Aging-Alzheimer's Association workgroups on diagnostic guidelines for Alzheimer's disease. Alzheimers Dement. 7, 280–292.
Taoka, T., Naganawa, S., 2020. Glymphatic imaging using MRI. J. Magn. Reson. Imaging 51, 11–24.
Taoka, T., Masutani, Y., Kawai, H., et al., 2017. Evaluation of glymphatic system activity with the diffusion MR technique: diffusion tensor image analysis along the perivascular space (DTI-ALPS) in Alzheimer's disease cases. Jpn. J. Radiol. 35, 172–178.
Taoka, T., Ito, R., Nakamichi, R., et al., 2022. Reproducibility of diffusion tensor image analysis along the perivascular space (DTI-ALPS) for evaluating interstitial fluid diffusivity and glymphatic function: CHanges in Alps index on multiple conditiON acquIsition eXperiment (CHAMONIX) study. Jpn. J. Radiol. 40, 147–158.
Tosun, D., Landau, S., Aisen, P.S., et al., 2017. Association between tau deposition and antecedent amyloid-β accumulation rates in normal and early symptomatic individuals. Brain 140, 1499–1512.

Villemagne, V.L., Fodero-Tavoletti, M.T., Masters, C.L., Rowe, C.C., 2015. Tau imaging: early progress and future directions. Lancet Neurol. 14, 114–124.
Weston, P.S.J., Simpson, I.J.A., Ryan, N.S., Ourselin, S., Fox, N.C., 2015. Diffusion imaging changes in grey matter in Alzheimer's disease: a potential marker of early neurodegeneration. Alzheimers Res. Ther. 7, 47.
Zeppenfeld, D.M., Simon, M., Haswell, J.D., et al., 2017. Association of Perivascular Localization of Aquaporin-4 with cognition and Alzheimer disease in aging brains. JAMA Neurol. 74, 91–99.